Zero-order controlled release of ciprofloxacin-HCl from a reservoir-based, bioresorbable and elastomeric device

Citation: Tobias, Irene S., Heejin Lee, George C. Engelmayr Jr., Daniel Macaya, Christopher J. Bettinger, and Michael J. Cima. "Zero-Order Controlled Release of Ciprofloxacin-HCl from a Reservoir-Based, Bioresorbable and Elastomeric Device." Journal of Controlled Release 146, no. 3 (September 15, 2010): 356–362.

As Published: http://dx.doi.org/10.1016/j.jconrel.2010.05.036

Publisher: Elsevier

Persistent URL: http://hdl.handle.net/1721.1/99418

Version: Author's final manuscript: final author's manuscript post peer review, without publisher's formatting or copy editing

Published in final edited form as:
J Control Release. 2010 September 15; 146(3): 356–362. doi:10.1016/j.jconrel.2010.05.036.

Zero-order controlled release of ciprofloxacin-HCl from a reservoir-based, bioresorbable and elastomeric device

Irene S. Tobias[a], **Heejin Lee**[b,g], **George C. Engelmayr Jr.**[c], **Daniel Macaya**[d], **Christopher J. Bettinger**[e], and **Michael J. Cima**[f,*]

[a] Department of Biological Engineering, Massachusetts Institute of Technology, Cambridge, MA 02139, USA

[b] Department of Mechanical Engineering, Massachusetts Institute of Technology, Cambridge, MA 02139, USA

[c] Harvard-M.I.T. Division of Health Sciences and Technology, Cambridge, MA 02139, USA

[d] Department of Materials Science and Engineering, Cornell University, Ithaca, NY 14850, USA

[e] Department of Materials Science and Engineering, Massachusetts Institute of Technology, Cambridge, MA 02139, USA

[f] Convergence Products Research Laboratory, Department of Materials Science & Engineering, Koch Institute of Integrative Cancer Research, Massachusetts Institute of Technology, 77 Massachusetts Ave., Rm 12-011, Cambridge, MA 02139, USA

Abstract

A reservoir-based device constructed of a completely biodegradable elastomer can enable many new implantation and insertion options for localized drug therapy, particularly in the case of urological therapies. We performed an *in vitro* performance evaluation of an implantable, bioresorbable device that supplies short-term controlled release of ciprofloxacin-HCl (CIP). The proposed device functions through a combination of osmosis and diffusion mechanisms to release CIP for short-term therapies of a few weeks duration. Poly(glycerol-*co*-sebacic acid) (PGS) was cast in a tubular geometry with solid drug powder packed into its core and a micro-machined release orifice drilled through its wall. Drug release experiments were performed to determine the effective release rate from a single orifice and the range of orifice sizes in which controlled zero-order release was the main form of drug expulsion from the device. It is demonstrated that PGS is sufficiently permeable to water to allow the design of an elementary osmotic pump for drug delivery. Indeed, PGS's water permeability is several orders of magnitude larger than commonly used cellulose acetate for elementary osmotic pumps.

Keywords

Elementary osmotic pump; Biodegradable polymers; PGS; Ciprofloxacin; Insertable devices

[*]Corresponding author. Tel.: 617 253 6877; fax: 617 258 6936 mjcima@mit.edu (M. J. Cima).
[g]Present address: TARIS Biomedical, Inc., 99 Hayden Ave. Ste 100, Lexington, MA 02421, USA

Introduction

Methods for controlled and sustained drug delivery for local urological applications are not known. These advantages include direct therapy to the target organ, continuous maintenance of target drug concentration, and potentially reduced toxicity [1,2]. Urology is a field in which minimally invasive techniques including catheterization, cystoscopy, and trans-rectal injection are available for device deployment into hollow, fluid-filled organs such as the bladder, uterus, or seminal vesicle. Some of these procedures are so minimally invasive that a device deployed in such a fashion might best be described at “insertable” rather than implantable. Urological drug delivery devices may be beneficial in situations where conventional treatments such as systemic oral administration routes and immediate drug release treatments have failed or become overly inconvenient and for which localized drug therapy is already being advocated. These situations involve indications such as interstitial cystitis, chronic prostatitis, non muscle invasive bladder cancer, and overactive bladder [3-6].

Biodegradable devices offer additional convenience and benefit by eliminating the need for a removal procedure. Devices that employ an osmotic pump to power drug release are capable of providing sustained, zero-order release over an extended period of time [7-12]. An elementary osmotic pump device constructed of an elastomeric, biodegradable polymer forming its semi-permeable membrane is particularly advantageous as an insertable drug delivery system for a urological indication.

The osmotic pump mechanism is driven by the diffusion of water through a semi-permeable membrane into a compartment containing an osmotic agent. The resulting pressure compresses a separate compartment that contains the drug solution and expels drug at a controllable rate through a release orifice [7-12]. If the orifice is too small, release is controlled by the pressure drop through the orifice. If the orifice is too large, release is controlled by simple bulk diffusion through the orifice. The desirable intermediate regime is one where the release rate is controlled by the permeation rate of water through the semi-permeable membrane. The release rate for an osmotic pump operating under these conditions is estimated by the equation

$$(dM/dt)_{osmosis} = C \cdot dV/dt = (A/h) \cdot k \cdot \Delta\pi \cdot C \qquad \text{(Eq. 1)}$$

where dM/dt is the drug mass release rate, dV/dt is the volume flux of a solvent (drug mass flux out is positive, solvent flux in is negative), $\Delta\pi$ is the osmotic pressure difference driving the water permeation, C is the concentration of drug in the dispensed fluid, k is the water permeability of the membrane, A is the membrane surface area and h is the membrane thickness using the standard osmotic theory assumptions described in prior work [11]. The elementary osmotic pump (EOP) first developed by Theeuwes in 1974 employs a solid drug as the osmotic agent [11]. The EOP has advantages over earlier osmotic pump designs in that it can often hold higher drug payloads and does not require a separate salt compartment [7,8]. The main drug release rate will remain zero-order providing the terms in Eq. 1 remain constant, a condition which can be controlled by optimizing the drug's solubility and the properties of the membrane [8,11]. The size of the delivery orifice must also be carefully selected to ensure that it will not interfere with the release rate. The orifice must be small enough to minimize bulk diffusion of the drug through the orifice but large enough so that the release rate is controlled by flux of water through the surface of the device rather than the pressure drop through the orifice [8,10,11].

Several previous osmotic pump implants have been constructed of non-degradable materials and have been limited to sub-cutaneous implantation due to their required removal

procedures [13-15]. A biodegradable osmotic pump would enable implantation in other disease sites where device retrieval is restricted. Ryu et al. have reported on a micro-osmotic pump constructed of poly(L-lactide-co-glycolide) (PLGA) [16]. The investigators report the water permeability of PLGA is only 1×10^{-21} m^2/Pa-s. The low permeability of PLGA and small size of the devices limited drug delivery rates of 20 to 40 ng/day in this demonstration. Biodegradable elastomers in such devices may have advantages over PLGA due to their more flexible nature and similarity to the mechanical properties of soft tissues [17-19]. This mechanical compatibility allows for enhanced physiological fit. Elastomeric properties also provide greater utility in device implantation for such techniques as catheterization or biopsy injection. Devices constructed from biodegradable elastomers have also been demonstrated to achieve sustained drug release [20,21]. These studies report on a reputed osmotic driven flux from drug embedded in a matrix of new biodegradable elastomer based on a photocrosslinked acrylated star copolymer macromer of ε-caprolactone and D,L lactide. In this method, drug and excipient is dispersed within the polymer matrix into micro regions. There is no hydraulic path from these regions to the surface of the device as their concentration is low enough to avoid percolation (typically lower than 10 vol %) and prevents rapid release of the drug. This low solids loading requirement again means a very small drug loading was achieved and the lack of osmotically driven hydraulic flow as in a conventional osmotic pump means that release rates will be very small unless the device is quite large.. *In vivo* performance of this photo crosslinked elastomer was not reported.

Our approach is to investigate a resorbable elastomer with a significant *in vivo* record and to construct a true elementary osmotic pump. This design framework will allow us to maximize drug payload by using the polymer on the exterior surface of the device with the interior volume composed only of drug. An exemplary elastomeric polymer is poly(glycerol-*co*-sebacic acid) (PGS), developed by Wang et al. in 2002 [22]. PGS has been shown to exhibit comparable or better biocompatibility than PLGA when tested *in vivo* [23-26]. Its previously shown *in vivo* properties (surface-eroding degradation, maintenance of mechanical strength, minimal host irritation, and negligible degree of fibrous encapsulation) [22,23] make it suitable for drug treatments including antibiotic therapy and post-surgical pain relief.

The drug payload used for this study is ciprofloxacin-HCL (CIP). CIP is a second generation fluoroquinolone antibiotic commonly used to treat a range of infections [27]. EOP devices for the release of CIP have been demonstrated in vitro [28] but were designed for oral use and not composed of resorbable materials.

Our current investigation is aimed at developing an antibiotic-releasing device to deploy into urological organs for treatment of chronic prostatitis over the course of three weeks. Thus, we have performed additional stability experiments monitoring the degradation of PGS in urological environments (synthetic urine, alkaline solution). Both the seminal vesicles and infected prostate glands are noted to be alkaline with a pH range of 7.8-8.3 [29-31]. The device can also be developed for other implantable therapies of similar time scale. The devices were fabricated with a micro-sized orifice and loaded with a solid drug core. Zero-order delivery of CIP was obswerved over the course of ten days as is described below.

2. Materials and Methods

2.1 Device Fabrication

An aluminum mold was designed and machined in-house to cast PGS into consistent, reproducible tubular modules of specified core size. The mold design consisted of a 76.2 × 25.4 × 12.7 mm aluminum bar (McMaster-Carr, Robbinsville, NJ) that was milled to a depth of 10.8 mm with 1-mm margins. Seven 340 μm diameter holes were drilled on both ends at

2.5 mm intervals with 2.5 μm tolerance to provide sockets for wire alignment. Steel wires (330 μm diameter, Small Parts, Inc, Miramar, FL) were strung through each pair of end sockets to produce the ~300 μm core of the modules, allowing for the swelling of PGS that occurs from rinsing procedures after removal from the mold. PGS pre-polymer was synthesized by polycondensation of 1.4 moles each of glycerol (Sigma-Aldrich, St. Louis, MO) and sebacic acid (Aldrich) at 130 °C under argon for 24 hours before reducing the pressure from 1 Torr to 40 mTorr. The reaction was maintained at 40 mTorr and 120 °C for 30 hours. The pre-polymer was cooled and stored in a desiccative environment at room temperature until further use. 4 g of the PGS pre-polymer was melted at 160 °C in the aluminum mold. The pre-polymer was cured at 135 °C and 50 mTorr for 48 hours (Fig. 1).

The orifice for osmotic drug delivery was drilled by excimer laser microablation using methods adapted from Engelmayr et al. [32]. A cured PGS slab (1.5 mm thick) within its mold was placed on the programmable x-y stage (accuracy ± 1 μm) of a Rapid X® 1000 excimer laser system (Resonetics, Nashua, NH). Desired pore diameters (e.g., 75, 100, and 150 μm) and layouts were patterned semi-automatically via a combination of a custom program developed in G-code and manual alignment of the laser to a paper template of the wire positions (Solidworks CAD software; SolidWorks, Concord, MA). The template was affixed with edges coincident to an in-house machined right-angle corner mount to assist in template-mold alignment. A power level of 350 mJ, burst frequency of 500/sec and burst count of 4000 were found to be suitable for complete microablation of the PGS down to the level of the stainless steel wire.

The mold was then soaked in de-ionized water (diH_2O) for 24 hours at 60 °C before removing the wires and PGS casting from the aluminum mold. The casting was serially placed in ethanol (Pharmco, Brookfield, CT) for 24 hours, diH_2O for 24 hours and then dried at 60 °C for 24 hours. The casting was roughly 1.5 mm thick and was cut by hand into modules with targeted dimensions of 10 mm × 1.5 mm × 1.5 mm, each containing a release orifice located about mid-length (Fig. 1). Control modules and 300 μm release modules did not contain a laser drilled orifice.

2.2 In Vitro PGS Degradation

A silicon wafer was spin-coated with sucrose solution to form a sacrificial release layer and 7 g ± 0.05 g of the PGS pre-polymer was melted and spread across the surface at 160 °C to form a 1 mm thick PGS sheet. The pre-polymer sheet was further cross-linked at 130 °C and 50 mtorr for 48 hours with a liquid nitrogen trap attached to the vacuum line. The PGS sheet was incubated in diH_2O for 24 hours to induce delamination from the wafer via sucrose dissolution. The sheet was removed from the wafer and placed overnight in ethanol, overnight in diH_2O and dried at 60 °C as described previously. Circular discs were cut from the sheet using an 8-mm diameter punch.

The PGS discs were weighed and deposited in pre-weighed 1.5 ml vials and immersed in 1 ml of 0.1 mM NaOH solution, pH~10. An additional line of PGS discs were weighed and placed in a 24-well plate and each was immersed in 1 mL of Surine^{TM} Negative synthetic urine, pH~7.4 (Dyna-Tek Industries, Lenexa, KS). All samples were placed on a rotator at low speed and incubated at 37 °C. Each week throughout a course of six weeks, all samples were re-suspended in NaOH solution or synthetic urine and a subsection of samples were withdrawn for assaying. Three discs of each type (PGS in NaOH and PGS in urine) were rinsed in 1 ml diH_2O and dried overnight at 60 °C in the assay protocol. The discs were then immersed in ethanol for 24 hours followed by immersion in diH_2O for 24 hours and drying overnight at 60 °C. The final dry weight of each sample was recorded to monitor degradation over time.

2.3 In vitro release experiments

Ciprofloxacin hydrochloride (Aurobindo Pharma Ltd, Hyderabad, India) (CIP) was loaded into the PGS modules through solid packing into rods of 3-5 mm in length (see supplementary info for details on drug rod casting and loading procedure). Steel wires of diameter 0.015 inches (380 μm) purchased from Small Parts Inc were used as plugs to prevent CIP from leaking through the module ends. The approximate average thickness of each module side and the diameter of each packed CIP rod was measured on an Axiovert 200 inverted light microscope (Carl Zeiss MicroImaging Inc, Thornwood, NY) at 2.5X using the measurement feature of the accompanying AxioVision 3.1 imaging software. The modules were each immersed in 2 mL diH_2O and stored at 37 °C. 1 mL of solution from each vial was withdrawn for concentration analysis and 1 mL of solution was replaced at each time point in order to approximate an infinite sink. The amount of CIP in each sample was determined using a quantitative HPLC-UV detection method for CIP adapted from USP.

An Atlantis T3 100 Å 250 mm × 4.6 mm, 5 μm column (Waters Corp, Milford, MA) was used with an eluting system consisting of acetonitrile (EMD Chemicals Inc, Darmstadt, Germany) as the mobile phase and 0.01 M phosphate buffer as the aqueous phase. The phosphate buffer consisted of a 2:1 molar ratio of sodium monophosphate (Mallinckrodt Baker, Inc., Phillipsburg, NJ) and phosphoric acid (Sigma Aldrich) titrated to pH 2.8. A gradient method was applied over 10 minutes with 20%:80% of mobile phase: aqueous phase at time 0 min., adjusted to 70% mobile phase by 8 min. and 20% mobile phase by 9 min. with a constant flow rate of 1 mL/min on an 1100 series HPLC solvent delivery system (Agilent Technologies, Santa Clara, CA). Detection was performed with a UV-visible detector set at 275 nm with an injection volume of 20 μL per sample. The limit of detection was approximately 50 ng/mL for ciprofloxacin in aqueous diluents and the retention time was around 5.6 minutes. CIP concentration standards ranging from 100 ng/ml to 30 mg/ml were used to construct a calibration curve. The modules were cut open at the end of each release experiment, and the drug content was extracted to determine the remaining CIP mass by HPLC-UV analysis.

3. Results

3.1 Device Fabrication

Photographs of PGS modules loaded with CIP-HCl are shown (Fig. 2B-2D). Each module was approximately 1 cm long and contained a CIP rod of variable packing density in the range of 3-5 mm in length. Measured thicknesses of the PGS wall were in the range of 250-1300 μm although the target thickness was 600 μm for a 1.5 mm thick module containing a 300 μm diameter core. The thicknesses were variable both between the sides of the same module and between different modules due to the deformability of the polymer during cutting. Each orifice for the modules used in the release experiments was checked for release function by fluid injection and showed no obstruction. Laser drilled orifice diameters were either 100 μm, 150 μm, or in the range of 70-90 μm for these modules.

3.2 In Vitro PGS Degradation

The *in vitro* degradation profile of PGS at 37 °C was tested in both synthetic urine and sodium hydroxide solution at pH ~10 over a time period of six weeks (Fig. 3) for the two conditions analyzed in which the average percent mass remaining (m/m_o, instantaneous mass/initial mass) among each triplicate of samples at each time point is plotted. Error bars are calculated as the standard deviation in m/m_o for each triplicate.

Mass retention did not drop below 75 % after 3 weeks or 70 % after six weeks. PGS exhibits more rapid initial degradation at higher pH as compared to physiological conditions due to base-catalyzed hydrolysis. Stable, linear mass loss is soon recovered however, with a comparable degradation rate to that observed at pH 7.4.

3.3 In vitro Release Experiments

Fig. 4 shows results from a representative release experiment of CIP from PGS modules containing a 100 μm orifice compared to a control module without an orifice. The initial drug payload for each module was calculated by the sum of the total drug amount released during the experiment and the remaining mass extracted from the module at the end of the experiment, both measured by HPLC-UV. An induction time is observed before the onset of zero-order controlled release kinetics during which water permeates into the devices and begins to dissolve some of the drug payload. The two 100 μm modules are observed to release CIP at nearly the same rate after induction even though one of the modules contained nearly three times the payload amount of the other. The smaller payload profile begins to flatten out once its CIP contents become fully dissolved and subsequently depleted.

Modules with different orifice sizes (70-90, 100, 150 and 300 μm in diameter) and control modules with no orifice were tested in release experiments to characterize the orifice size regime that would provide zero-order, payload-independent drug release. CIP release profiles were collected for each module and plotted as cumulative drug mass released vs. time after osmotic induction (Fig. 5). The release rate for each profile portrayed in Fig. 5 was multiplied by the average PGS wall thickness measured for each module and plotted for each timepoint after induction (Fig. 6).

The 100 and 150 μm profiles shown in Fig. 5 and Fig. 6 illustrate zero-order kinetics of CIP release from the PGS modules, as the total drug amount released exhibits a linear relationship with time for most of the drug mass released from each payload. The release rate remains roughly constant over time during release of up to 90% of the drug payload for these modules, as shown in Fig. 6. The rate then decreases as the payload becomes fully dissolved, as seen in the leveling of the profiles in Fig. 5 that approach completion of their payload release. The rate of drug release through 100 and 150 μm orifices for most of the drug mass released in these profiles is also independent of initial payload, as each module in this class released CIP at roughly the same rate even though some had 2-3 times the payload of others. The water permeability (k) of PGS was estimated to be in the range of 3.9-6.5 × 10^{-17} m^2/Pa·sec using the data from these modules. The value of $k^*\Delta\pi$ in the work of Theeuwes [11] for the cellulose acetate used as the semipermeable membrane was measured as 0.686 × 10^{-3} cm^2/hr, which calculates k to be 7.7 × 10-^{19} m^2/Pa·sec using the osmotic pressure of potassium chloride at 37 °C (245 atm) [12].

The portion of the release rate due to diffusion was also estimated for these modules by applying the following

$$(dM/dt)_{diffusion} = D_{cip} \cdot C_{cip} \cdot \left(A_{orf}/h\right) \quad \text{(Eq. 2)}$$

where D_{cip} is the diffusion coefficient of CIP in water (D_{cip} = 4.9 × 10^{-6} cm^2/sec) [33], C_{cip} is the solubility of CIP-HCl in water (C_{cip} = 30 mg/ml) [34], A_{orf} is the surface area of the orifice and h is the average PGS wall thickness, assuming infinite sink conditions. The release rate due diffusion was estimated to be 26-33% and 65-68% of the total drug release rate for the 100 μm and 150 μm orifice modules, respectively.

The release rate from 300 μm orifices is payload-dependent, as initial release rates were variable among different drug payloads. The shapes of most of the 300 μm profiles (with the possible exception of the 427 μg payload) also suggest a more dominant diffusion release mechanism as they express significantly less linearity than the 100 μm and 150 μm profiles. The release rate for each module is shown to decline over time during the majority of the payload release (Fig. 6) thus implicating that 300 μm orifices do not permit osmotic control for zero-order release kinetics by allowing significant payload-dependent diffusion processes to occur.

Drug release from the control modules without an orifice is the result of CIP diffusion through either the PGS wall or any potential gaps between the PGS and the wire plugs. The control module drug release is measured to be approximately 4% of the release rate through the 100 μm orifices. This release rate is also zero-order and is driven by both a constant osmotic pressure gradient and a high, roughly constant concentration gradient which push CIP molecules through micro-gaps in the PGS matrix.

Fig. 5 also suggests that 150 μm orifices release CIP at a slightly faster rate than 100 μm orifices. The thickness (*h*) of a semi-permeable membrane has a direct inverse relationship to drug release rate for both osmotic and diffusion components, as noted in Eq. 1 and Eq. 2. Wall thicknesses were measured for each module and were noted to be thinner for modules expressing a faster release rate among the 100 and 150 μm modules. Fig. 6 accounts for this variability, and thus multiplies the release rate for each module by its average measured thickness. Modules with 150 μm orifices are thus shown to release CIP at a comparable rate to those with 100 μm orifices. Modules with orifices of diameter in the range of 70-90 μm have slower release rates than the modules with 100 μm orifices, particularly in the case of the 70 μm orifice. These orifice sizes exist in a size regime where release rate is not independent of orifice size.

The average release rate measured among the six modules with 100 μm or 150 μm orifices was 2.45 ± 0.36 μg/hour. Induction times for drug release among modules were also variable, generally ranging between 12 and 48 hours with two exceptions at 63 and 82 hours which were attributed to higher packing of drug powder within the orifice channel. Drug release was thus inhibited until the orifice was cleared of solid drug by dissolution.

4. Discussion

In vitro degradation experiments suggest that PGS degrades hydrolytically through a surface eroding mechanism at the thickness scale of the proposed device (1-2 mm). PGS is shown to lose mass linearly over time in both urine and NaOH solution, a characteristic feature of surface eroding polymers [35,36]. This surface-eroding behavior concurs with previously reported studies of PGS cured to a lower crosslink density via a lower applied pressure and temperature (30 mTorr, 120°C for 48 hours) which was shown to swell negligibly in water and degrade via surface erosion [22,23].

The surface eroding property of PGS also allows the crosslink density of the polymer to remain roughly constant while the molecules at the surface degrade. The diffusion coefficient of CIP in bulk PGS thus remains constant, as shown by the slow zero-order release of CIP through the PGS wall of the control modules without an orifice (Fig. 5, Fig. 6). The release kinetics should accelerate at longer times when significant PGS surface erosion into the core of the device has occurred. Optimal design of a drug delivery device would be one where the entire drug payload has released before degradation of the PGS. The degradation experiments also suggest that PGS can sustain a sufficient percentage of its mass to function as a drug releasing device of 1-2 mm thickness over a time period of a few

weeks in both urine and NaOH. *In vivo* degradation will be substantially accelerated by the activity of surface eroding enzymes however, and will limit the use of this device to short-term drug therapies [23].

In vitro release experiments demonstrate that a prototype EOP for controlled drug release can be constructed from a hydrophobic bio-resorbable polymer that is also shown to be surface eroding at the length scale of the device. The permeation of water through a 0.2-1 mm thick PGS membrane is sufficient to enable osmotically-driven drug release and is not functionally inhibited by the polymer's hydrophobicity at this length scale. The PGS membrane is also shown to have a semipermeable nature, as drug permeation through the walls of the control modules which lack an orifice is shown to be negligible in comparison to drug release through an orifice. However, the current rudimentary device fabrication procedure lacks the precision to form a specified and uniform PGS membrane thickness (*h*), thus limiting the precision and reproducibility of the directly-dependent release rate (*dM/dt*). In addition, the steel wires used to seal the ends of the device will need to be replaced by microspheres composed of a stiff bioresorbable material such as PLGA or PLA in order for the device to be fully resorbable. This change to the device should not affect its elastomeric properties or release performance as long as the resorbable material functions in preventing the leakage of drug.

The results of these experiments concur with osmotic pump theory in that zero-order release kinetics were demonstrated for devices containing an orifice of the appropriate diameter (100-150 μm) in which the release rate was independent of orifice size. These results are similar to the range of orifice size eliciting zero-order release kinetics reported by Theeuwes, which was 75-274 μm for a potassium chloride EOP [11]. Estimates for the portion of the drug release rate due to diffusion from the 100 and 150 μm devices suggested that diffusion effects were still significant even though zero-order release was attained. This result is likely due to the low solubility of ciprofloxacin-HCl (30 mg/ml) [34], permitting the maintenance of a saturated drug solution within the device core. The saturated drug solution provides a constant driving force for drug diffusion in addition to the constant osmotic pressure resulting in a combined mechanism for zero-order drug release. In the case of the non-linear release profiles noted for the 300 μm orifice devices, drug diffusion is likely fast enough that a constant, saturated concentration gradient cannot be maintained within the device.

Ciprofloxacin hydrochloride was also shown to function well as the active osmotic drug agent in the device core without need for co-formulation with agents of higher osmotic activity. CIP's low solubility in water can hinder certain processing methods such as solution casting, yet it improves the extended zero-order behavior of the drug release profile as the payload remains un-dissolved for a greater proportion of the release time period. The drug release rate could be increased as needed by incorporating multiple reservoirs/orifices modules while the treatment period can be extended by increasing the length of the device payload.

One potential application for an enhanced version of this device could be the treatment of chronic prostatitis (CP). This condition is common in men (approximate prevalence of 10%) [37] and is typically treated with ciprofloxacin or other fluoroquinones [38]. Furthermore, local antibiotic therapy involving intraprostatic injections has been advocated to achieve enhanced clinical efficacy in patients for which systemic antibiotic therapy has failed [4,5]. A device could potentially be implanted into the seminal vesicle via transrectal needle injection to release an antibiotic drug into the nearby prostate gland for a period of 2-4 weeks (a typical course of treatment for CP) [39]. A proposed version of the device for this application, containing 8.0 - 8.5 mg of CIP, could be 2.5 cm in length with 500-μm thick

walls, a 450-μm diameter drug rod and a single 100-μm diameter orifice. This device would fit within a 14 gauge (1.6 mm inner diameter) transrectal needle for injection into the torturous inner tubule of the seminal vesicle (2-6 mm in diameter in the normal male) [40]. Using the direct relationships of release rate (*dM/dt*) with wall thickness (*h)* and length (proportional to *A*) from Eq. 1, the estimated release rate for this device is 16.6 ± 2.5 μg/hr. This rate corresponds approximately to 4 μg/ml of CIP per hour into the 3-4 ml fluid capacity of the seminal vesicle [41] and would be capable of killing most species of gram-negative bacteria responsible for CP (Minimal Inhibitory Concentration of 0.005 μg/ml - 0.8 μg/ml for CIP) [42].

5. Conclusions

The *in vitro* testing of the proposed device's performance has demonstrated functionality and stability of the device. Resorbable, elastomeric PGS was shown to effectively function as a semi-permeable material for an elementary osmotic pump to achieve controlled release of ciprofloxacin. Orifices with diameters of 100-150 μm were found to allow zero-order release kinetics for which release rate was independent of orifice size.

Supplementary Material

Refer to Web version on PubMed Central for supplementary material.

Acknowledgments

This research was funded by the Deshpande Center for Technological Innovation at Massachusetts Institute of Technology. H. Lee acknowledges additional support from the Samsung Scholarship from the Samsung Foundation of Culture.

References

1. Langer R. Implantable Controlled Release Systems. Pharm. Ther. 1982; 21:35–51.
2. Sershen S, West J. Implantable, polymeric systems for modulated drug delivery. Adv. Drug Deliv. Rev. 2002; 54:1225–35. [PubMed: 12393303]
3. Henry R, Patterson L, Avery N, Tanzola R, Tod D, Hunter D, et al. Absorption of alkalized intravesicle lidocaine in normal and inflamed bladders: a simple method for improving bladder anesthesia. J. Urology. 2001; 165:1900–1903.
4. Yamamoto M, Hibi H, Satoshi K, Miyake K. Chronic bacterial prostatitis treated with intraprostatic injection of antibiotics. Scand. J. Urol. Nephrol. 1996; 30:199–202. [PubMed: 8837251]
5. Guercini F, Pajoncini C, Bard R, Fiorentino F, Bini V, Costantini E, Porena M. Echoguided drug infiltration in chronic prostatitis: results of a multi-centre study. Arch. Ital. Urol. Androl. 2005; 77:87–92. [PubMed: 16146268]
6. Fowler CJ. Intravesicle treatment of overactive bladder. Urology. 2000; 55:60–64. [PubMed: 10767456]
7. Santus G, Baker RW. Osmotic drug delivery: a review of the patent literature. J. Control. Release. 1995; 35:1–21.
8. Verma RK, Mishra B, Garg S. Osmotically Controlled Oral Drug Delivery. Drug Dev. Ind. Pharm. 2000; 26:695–708. [PubMed: 10872087]
9. Ranade VV. Drug delivery systems. 4. Implants in drug delivery. J. Clin. Pharm. 1990; 30:871–89.
10. Verma RK, Krishna DM, Garg S. Formulation aspects in the development of osmotically controlled oral drug delivery systems. J. Control. Release. 2002; 79:7–27. [PubMed: 11853915]
11. Theeuwes F. Elementary Osmotic Pump. J. Pharm. Sci. 1975; 64:1981–87. [PubMed: 1206494]
12. Verma RK, Arora S, Garg S. Osmotic Pumps in Drug Delivery. Crit. Rev. Ther. Drug Carrier Syst. 2004; 21:477–520. [PubMed: 15658934]

13. Wright JC, Leonard ST, Stevenson CL, Beck JC, Chen G, Jao R, et al. An in vivo/in vitro comparison with a leuprolide osmotic implant for the treatment of prostate cancer. J. Control. Release. 2001; 75:1–10. [PubMed: 11451492]

14. Fisher DM, Kellett N, Lenhardt R. Pharmacokinetics of an implanted osmotic pump delivering sufentanil for the treatment of chronic pain. Anesthesiology. 2003; 99:929–37. [PubMed: 14508328]

15. Djalilian HR, Caicedo E, Lessan K, Grami V, Le CT, Spellman SR, et al. Efficacy of an osmotic pump delivered, GM-CSF-based tumor vaccine in the treatment of upper aerodigestive squamous cell carcinoma in rats. Cancer Immunol. Immunother. 2007; 56:1207–14. [PubMed: 17219150]

16. Ryu W, Huang Z, Prinz FB, Goodman SB, Fasching R. Biodegradable micro-osmotic pump for long-term and controlled release of basic fibroblast growth factor. J. Control. Release. 2007; 124:98–105. [PubMed: 17904240]

17. Amsden B. Curable, biodegradable elastomers: emerging biomaterials for drug delivery and tissue engineering. Soft Matter. 2007; 3:1335–48.

18. Bruggeman JP, Bettinger CJ, Nijst CLE, Kohane DS, Langer R. Biodegradable Xylitol-Based Polymers. Advanced Materials. 2008; 20:1922–27.

19. Bettinger CJ, Bruggeman JP, Borenstein JT, Langer RS. Amino alcohol-based degradable poly(ester amide) elastomers. Biomaterials. 2008; 29:2315–25. [PubMed: 18295329]

20. Gu F, Neufeld R, Amsden B. Osmotic-Driven Release Kinetics of Bioactive Therapeutic Proteins from a Biodegradable Elastomer are Linear, Constant, Similar, and Adjustable. Pharm. Res. 2006; 23:782–89. [PubMed: 16550470]

21. Gu F, Neufeld R, Amsden B. Sustained release of bioactive therapeutic proteins from a biodegradable elastomeric device. J. Control. Release. 2007; 117:80–89. [PubMed: 17126945]

22. Wang Y, Ameer GA, Sheppard BJ, Langer R. A tough biodegradable elastomer. Nat. Biotechnol. 2003; 20:602–06. [PubMed: 12042865]

23. Wang Y, Kim YM, Langer R. In vivo degradation characteristics of poly(glycerol sebacate). J. Biomed. Mater. Res. A. 2003; 66:192–97. [PubMed: 12833446]

24. Motlagh D, Yang J, Lui KY, Webb AR, Ameer GA. Hemocompatibility evaluation of poly(glycerol-sebacate) in vitro for vascular tissue engineering. Biomaterials. 2006; 27:4315–24. [PubMed: 16675010]

25. Bettinger CJ, Weinber EJ, Kulig KM, Vacanti JP, Wang Y, Borenstein JT, Langer R. Three-Dimensional Microfuidic Tissue-Engineering Scaffolds Using a Flexible Biodegradable Polymer. Advanced Materials. 2006; 18:165–69. [PubMed: 19759845]

26. Kim MS, Ahn HH, Shin YN, Cho MH, Khang G, Lee HB. An in vivo study of the host tissue response to subcutaneous implantation of PLGA- and/or porcine small intestinal submucosa-based scaffolds. Biomaterials. 2007; 28:5137–43. [PubMed: 17764737]

27. Samanidou VF, Demetriou CF, Papadoyannis IN. Direct Detection of four fluoroquinolones, enoxacin, norfloxacin, ofloxacin and ciprofloxacin, in pharmaceuticals and blood serum by HPLC. Anal. Bioanal. Chem. 2003; 375:623–29. [PubMed: 12638045]

28. Vyas SP, Guleria R, Singh R. Development and *In-Vitro* Characterization of Elementary Osmotic Pump Bearing Ciprofloxacin Hydrochloride. Eastern Pharmacist. 1996:167–69.

29. Ndovi TT, Choi L, Caffo B, Parsons T, Baker S, Zhao M, et al. Quantitative assessment of seminal vesicle and prostate drug concentrations by use of a noninvasive method. Clin. Pharm. & Ther. 2006; 80:146–58.

30. Anderson RU, Fair WR. Physical and chemical determinations of prostatic secretion in benign hyperplasia, prostatitis, and adenocarcinoma. Invest. Urol. 1976; 14:137–40. [PubMed: 61187]

31. Blacklock NJ, Beavis JP. The response of fluid pH in inflammation. Br. J. Urol. 1978; 46:537–42. [PubMed: 4609006]

32. Engelmayr GC Jr, Cheng M, Bettinger CJ, Borenstein JT, Langer R, Freed LE. Nat. Mater. 2008; 7:1003–10. [PubMed: 18978786]

33. Vranny JD, Steward PS, Suci PA. Comparison of Recalcitrance to Ciprofloxacin and Levofloxacin Exhibited by *Psudomonas aeruginosa* Biofilms Displaying Rapid-Transport Characteristics. Antimicrob. Agents and Chemother. 1997; 41(6):1352–58. [PubMed: 9174198]

34. Melo, MJP.; Varanda, FR.; Dohrn, R.; Marrucho, IM. Solubility of Ciprofloxacin and Moxifloxacin in Different Solvents: the Effect of the HCl Group. 2cd Mercosur Congress on Chemical Engineering; 2005.

35. von Burkersroda F, Schedl L, Göpferich A. Why degradable polymers undergo surface erosion or bulk erosion. Biomaterials. 2002; 23:4221–31. [PubMed: 12194525]

36. Göpferich A, Langer R. The influence of microstructure and monomer properties of the erosion mechanism of a class of polyanhydrides. J. Polym. Sci. A: Polym. Chem. 1993; 31:2445–58.

37. Schaeffer AJ, Wendel EF, Dunn JK, Grayhack JT. Prevalence and significance of prostatic inflammation. J. Urol. 1981; 125:215–19. [PubMed: 7206060]

38. Nickel, JC. Inflammatory Conditions of the Male Genitourinary Track: Prostatitis and Related Conditions, Orchitis, and Epididymitis. In: Wein, AJ.; Kavoussi, LR.; Novick, AC.; Partin, AW.; Peters, CA., editors. Campbell-Walsh Urology. 9th ed. Elsevier; Philadelphia: 2007. p. 304-29.

39. Bjerklund Johansen TE, Grüneberg RN, Guiber J, Hofstetter A, Lobel B, Naber KG, Palou Redorta J, van Cangh PJ. The Role of Antibiotics in the Treatment of Chronic Prostatitis: A Consensus Statement. Eur. Urol. 1998; 34:457–66. [PubMed: 9831786]

40. Older RA, Watson LR. Ultrasound Anatomy of the Normal Male Reproductive Tract. J. Clin. Ultrasound. 1996; 24:389–404. [PubMed: 8884518]

41. Sandlow, JI.; Winfield, HN.; Goldstein, M. Surgery of the Scrotum and Seminal Vesicles. In: Wein, AJ.; Kavoussi, LR.; Novick, AC.; Partin, AW.; Peters, CA., editors. Campbell-Walsh Urology. 9th ed. Elsevier; Philadelphia: 2007. p. 1098-1128.

42. Chin N, Neu H. Ciprofloxacin, a quinolone carboxylic acid compound active against aerobic and anaerobic bacteria. Antimicrob. Agents Chemother. 1984; 25:319–26. [PubMed: 6232895]

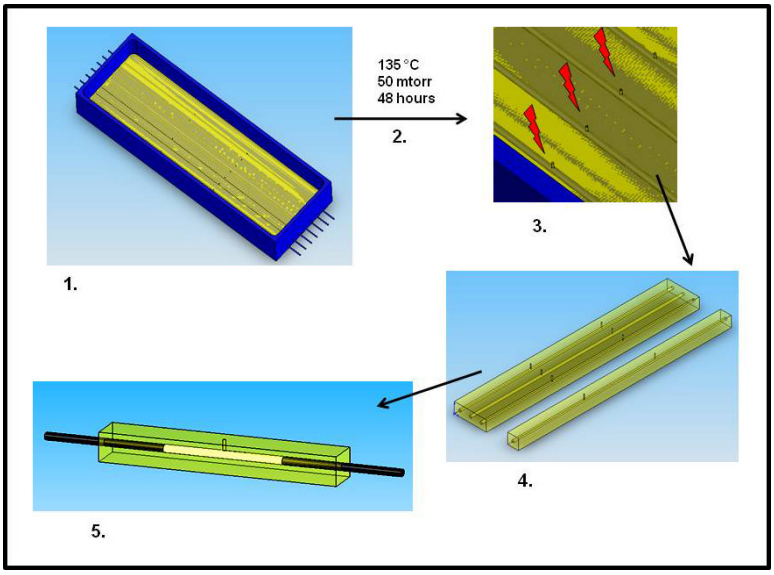

Fig. 1.

Device fabrication process (schematic not drawn to scale). 1) PGS pre-polymer is melted in an aluminum mold strung with wires to produce hollow cores for drug loading. 2) The pre-polymer is cross-linked under heat and vacuum for 48 hours. 3) A laser microablation method is used to drill release orifices in the top of the casting with wires left in place. Red marks indicate the positions of laser drilled holes. 4) The casting is removed from the mold and cut into rectangular modules. 5) Drug powder is loaded into the module which is plugged with stainless steel wires for use in release experiments.

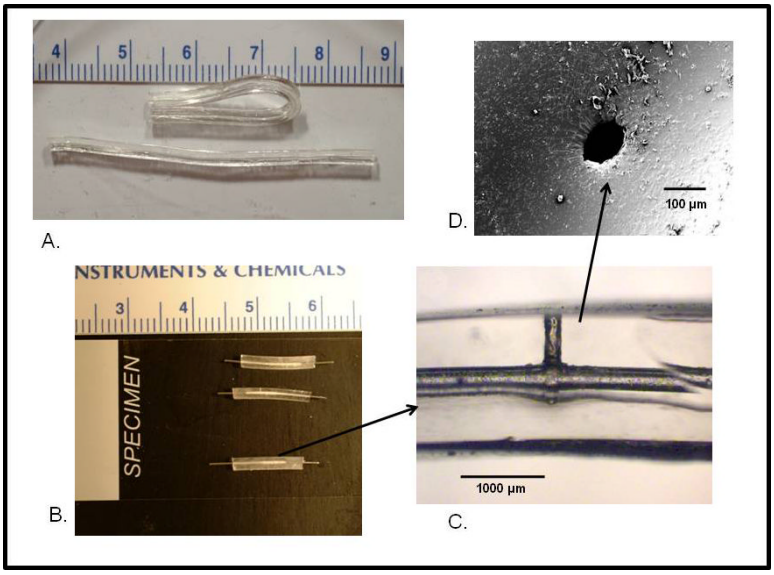

Fig. 2.

PGS castings. A) PGS tubes demonstrating flexibility of material. B) Sample PGS modules loaded with CIP and plugged with steel wires. C) Zoomed-in view of PGS module containing 150 µm diameter laser drilled orifice channel leading into 300 µm diameter core. D) SEM image of 100 µm diameter laser drilled orifice viewed from the orifice surface.

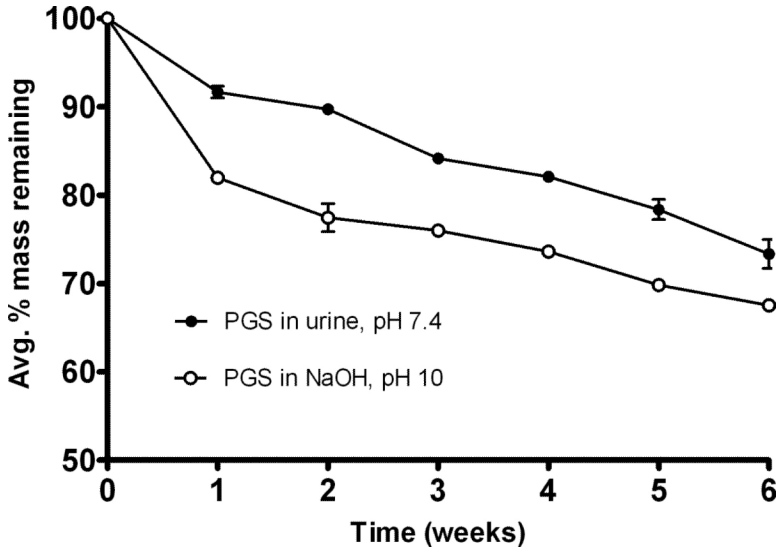

Fig. 3.

Degradation profiles of PGS discs incubated in different pH conditions. The average percent mass remaining of each disc is plotted over time. Error bars represent standard deviation, n = 3.

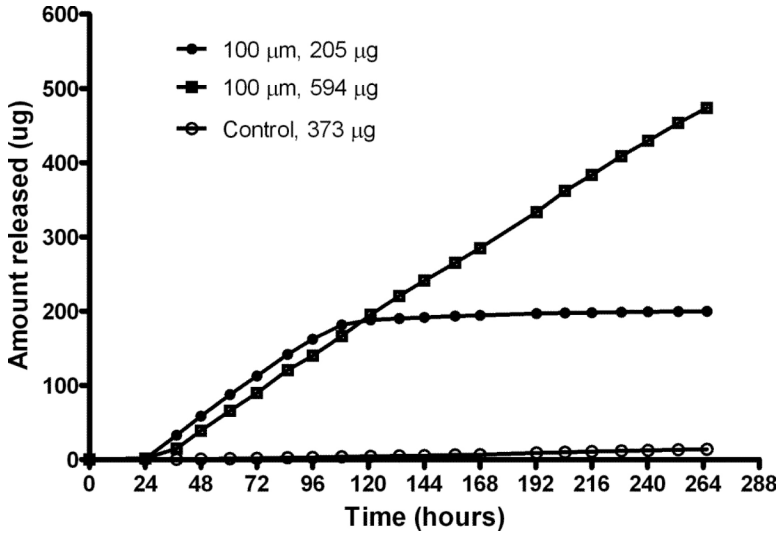

Fig. 4.

Representative ciprofloxacin release profiles from an experiment with 100 μm orifices in PGS modules. Cumulative amount released is plotted vs. time after immersion in DI-H_2O. The payload for each module is noted in μg. The control module did not contain an orifice.

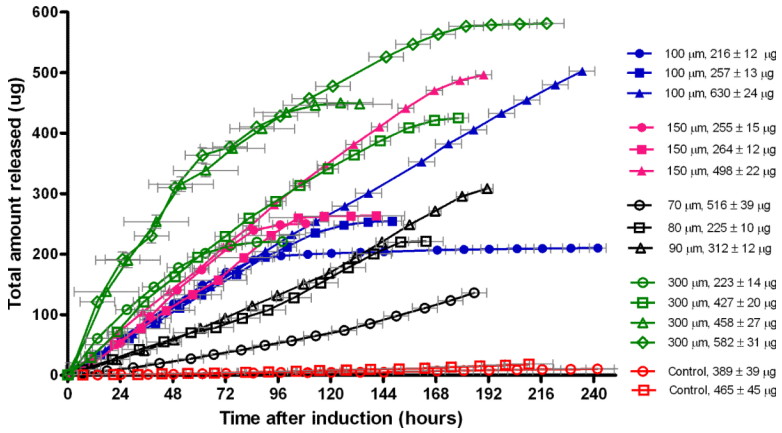

Fig. 5.

Release profiles of ciprofloxacin from PGS modules with orifices of differing size. The induction time was subtracted from each release profile. Induction times were calculated through extrapolation via linear fitting of the first three points from the release regime of each profile. Orifice diameter is noted in μm and initial drug payload is noted in μg for each drug-loaded module. Horizontal error bars represent error in induction time which was calculated by least squares fitting error analysis. Vertical error bars represent accumulated error of HPLC calibration, and sample dilution.

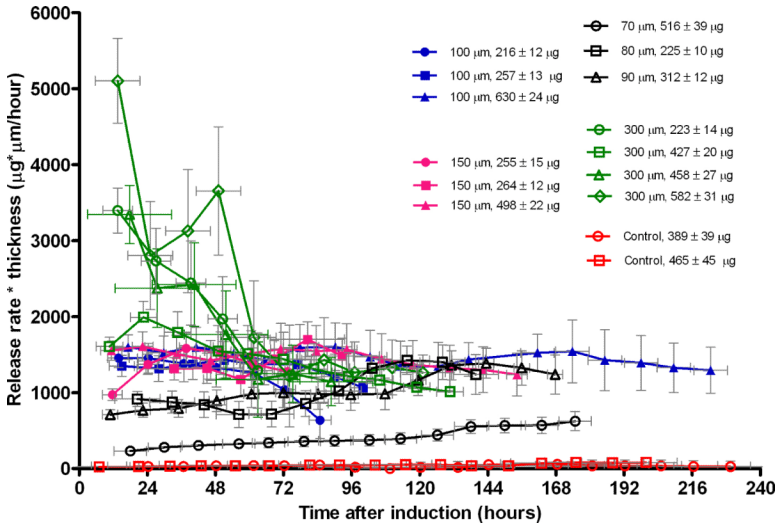

Fig. 6.

[Release rate*(average PGS wall thickness)] vs. time after induction for CIP-loaded PGS modules with different sized orifices. Release rate for each time point after induction was calculated as the slope of a three point moving average. Error in rate was calculated by least squares fitting error analysis. Rates were plotted for time points that corresponded up to 90% amount released of the total drug payload. Errors in drug payload were calculated by the accumulated error in CIP amount released from each time point in a profile. The average thickness of the three sides exposed to water for each PGS module was multiplied by the release rate at each time point.